Numerical analysis of deuterium migration behaviors in tungsten damaged by fast neutron by means of gas absorption method

Makoto I. Kobayashi[a,b], Masashi Shimada[c], Chase N. Taylor[c], Yuji Nobuta[d], Yuji Hatano[e] and Yasuhisa Oya[f]

[a]*National Institute for Fusion Science, National Institutes of Natural Sciences, 322-6 Oroshi, Toki, Gifu, Japan*
[b]*The Graduate University for Advanced Studies, SOKENDAI*
[c]*Idaho National Laboratory*
[d]*Hokkaido University*
[f]*Hydrogen Isotope Research Center, University of Toyama, Toyama, Japan*
[g]*Shizuoka University*

Deuterium retention behavior in tungsten damaged by fast neutrons at high temperatures (0.43 dpa at 918 K and 0.74 dpa at 1079 K) and 6.4 MeV Fe^{2+} (0.3 dpa at R.T.) were investigated to evaluate the tritium retention property of fusion reactor divertors. A deuterium gas absorption method was carried out to avoid additional damage that may be induced by plasma exposure, then, deuterium retention and desorption behaviors were investigated quantitatively by means of thermal desorption spectroscopy and the following simulation code. The deuterium desorption spectra for tungsten samples were analyzed by the numerical code which includes the elementary steps of hydrogen isotope migration processes including diffusion, trapping, detrapping, and surface recombination. The evaluated deuterium detrapping energy from the irradiation defects in neutron irradiated tungsten sample was larger than that in 6.4 MeV Fe^{2+} irradiated tungsten. It was suggested that the dominant deuterium trapping site in the neutron irradiated tungsten would be voids which was formed by the accumulation of vacancies during neutron irradiation under high temperature and long duration.

Keywords: tungsten, neutron, divertor, TDS.

1. Introduction

Tungsten is an attractive material for the application as a plasma facing material in a D-T fusion reactor, where the plasma facing materials are exposed to high heat flux, neutrons, and plasma of helium and hydrogen isotopes including tritium, due to its characteristics such as high melting point, low sputtering rate, and low hydrogen solubility [1-3]. For this application, hydrogen isotope retention behaviors in tungsten have been studied [4-6]. Hydrogen solubility and diffusivity in tungsten were investigated widely, and a low tritium inventory in tungsten wall was expected. However, the experimental research performed in the framework of the US-Japan joint research project PHENIX and TITAN showed a significant increase of hydrogen isotope retention in neutron irradiated tungsten [7-10]. Also, the desorption temperature of hydrogen isotopes shifted toward high temperature. These results indicate that the irradiation defects generated by neutron irradiation work as trapping sites for hydrogen isotopes in tungsten, and detrapping of hydrogen isotopes from these irradiation defects requires higher activation energy. In particular for neutron irradiation, irradiation defects distribute over an entire depth of tungsten, leading to a drastic increase of tritium inventory in tungsten.

From these experimental results, the evaluation of tritium retention in neutron irradiated tungsten should be necessary for estimating the fuel cycle of fusion reactor and the hazard potential in the case of accident such as LOVA (Loss of vacuum accident) [11-12]. For this purpose, the kinetics of trapping and detrapping processes of hydrogen isotopes in irradiation defects should be evaluated, and a comprehensive model including all elementary steps of hydrogen isotope migration in tungsten with irradiation defects should be achieved.

Our previous study attempted to model the hydrogen isotope migration in neutron irradiated tungsten [13]. This model roughly demonstrated the deuterium desorption behavior of neutron irradiated tungsten after deuterium plasma exposure. On the other hand, it is well known that high flux of deuterium plasma might induce the blistering structure on the surface of tungsten due to the excess deuterium solution [14-15]. Also, neutron irradiation in the previous study was carried out in the HFIR (High Flux Isotope Reactor), which is a nuclear fission reactor, in ORNL (Oak Ridge National Laboratory). The neutron spectrum in this irradiation included a large component of thermal neutrons, although a portion of the thermal neutrons would be much lower in the actual fusion reactor. Consequently, the population of transmuted elements in tungsten in the previous experiment was significantly different from the actual fusion reactor environment.

Therefore, we improved the irradiation capsule to use gadolinium (Gd) which works to absorb thermal neutrons [16]. Using this capsule, the neutron irradiation mainly with fast neutrons in HFIR was carried out into tungsten at the temperature above 1000 K in this study. This irradiation temperature is almost equivalent to the steady-state divertor operation temperature in DEMO [17]. Then, deuterium gas absorption was conducted in INL (Idaho National Laboratory) to induce deuterium into tungsten avoiding the above-mentioned surface morphology changes by high-flux deuterium plasma exposure. Thereafter, deuterium retention and desorption behavior

author's email: kobayashi.makoto@nifs.ac.jp

were investigated by means of thermal desorption spectroscopy (TDS). The deuterium distribution during the deuterium gas absorption and the TDS experiment were analyzed numerically by the comprehensive kinetic model of deuterium migration in tungsten with irradiation defects. Eventual deuterium retention and desorption behavior were reproduced by this model to deduce the trap density and the detrapping energy of deuterium from the irradiation defects.

2. Experimental

ITER grade polycrystalline tungsten samples (99.99% purity) purchased from Allied Material (A.L.M.T.) Corp. Ltd. were used in this study. The disc-shaped samples have been prepared by cutting polycrystalline tungsten rod and annealed at 1173 K for 1 h in a hydrogen atmosphere to relieve internal stresses in the manufacturing process. The diameter and the thickness of these samples were 6 mm^{φ}, and 0.25 mm^{t}, respectively. The samples were mechanically polished to mirror finish, and then annealed at 1173 K for 0.5 h in ultra-high vacuum (~10^{-6} Pa) [7, 18]. The details of sample preparation are described elsewhere [9]. Neutron irradiation was carried out in HFIR at ORNL. The neutron fluence and irradiation temperature were varied by the position of the capsule. In this study, two tungsten samples which were irradiated with fast neutron under the nominal temperatures of 918 and 1079 K were used. The damage levels were 0.43 and 0.74 dpa (displacement per atom), respectively. The damage level here was estimated by the fast neutron fluence.

For the comparison to the neutron irradiated sample, and for understanding the deuterium migration behaviors in bulk-damaged tungsten, heavy ion irradiation was also performed using accelerator DuET at Kyoto University [19]. The 6.4 MeV Fe^{2+} was irradiated into the tungsten sample up to the damage level of 0.3 dpa under room temperature. The damage rate was evaluated by the same manner as [20]. The depth distribution of irradiation defects was estimated by SRIM (Stopping Range of Ions in Matter) code as about 1.2 μm [21].

Thereafter four samples (0.43 and 0.74 dpa by neutron, 0.3 dpa by 6.4 MeV Fe^{2+}, un-damaged tungsten samples) were taken to INL for the post-irradiation experiments. Deuterium gas absorption was conducted on these samples in SGAP (static gas absorption and permeation) apparatus which is the system similar to TGAP (Tritium gas absorption and permeation) except the inability of tritium handling and the ability of deuterium absorption implementation [22]. The samples were installed into the single-end quartz tube. After the evacuation of the tube around 10^{-5} Pa, the sample temperature was increased by the furnace surrounding the tube up to 873 K. Then, deuterium gas was introduced into the tube to start the exposure. The deuterium gas was of 99.4% isotopic purity and the pressure was 80 kPa. The temperature of the furnace was decreased to the room temperature at the end of the daily experiment for laboratory safety requirement, and the temperature increased to 873 K again at the start of the daily experiment. The entire history of exposure temperature is displayed in Fig. 1. The heating and cooling of furnace was implemented as quickly as possible. The pressure of deuterium gas remained nominally constant in this deuterium gas exposure. The exposure time was close to 20 hours in total.

After the deuterium gas exposure, the samples were taken out from the SGAP apparatus, and installed one by one into the TDS system. TDS experiments were carried out in the heating rate of 10 K/min in the temperature range of room temperature to 1273 K. After reaching the temperature of 1273 K, this temperature was maintained for 30 min. The desorbed gas species during TDS were measured using a quadrupole mass spectrometer (QMS). In particular, the gas molecules including deuterium such as HD (mass 3), D_2 (mass 4), and HDO (mass 19) were monitored. The QMS signal of D_2 was calibrated by a D_2 gas bottle with a calibrated supply-rate. Also, the calibrations for other molecules containing deuterium such as HD and HDO were carried out where the ionization efficiency of HD was deduced as the average ionization efficiencies of H_2 and D_2, and the ionization efficiency of HDO was the same as that of H_2O. The analysis hereafter will be focused on the total deuterium desorption rate which is the sum of deuterium atom desorbed from all deuterium-containing molecules.

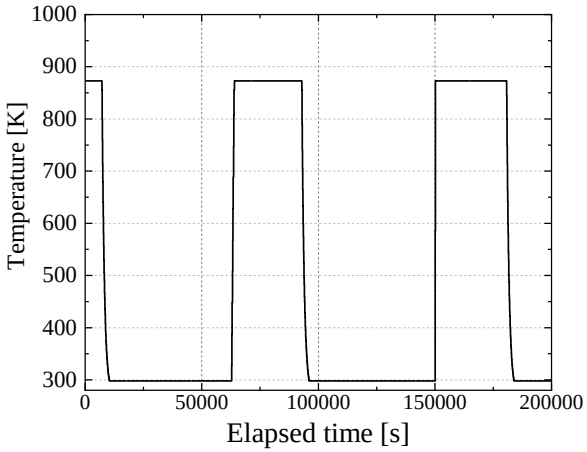

Fig. 1 Temperature history during deuterium gas absorption in this study. The pressure of deuterium gas hardly changed in this duration.

3. Simulation code

The time-evolution of deuterium distribution in tungsten samples was estimated by the developed simulation code. The code solves the one-dimensional McNabb-Foster equation for deuterium in tungsten containing trapping sites [23]. The detail of this code can be found elsewhere [24-25]. The kinetic parameters for the elementary steps of deuterium migration in tungsten, such as diffusion and recombination processes, were the same as our previous study [24]. Unlike these parameters, the detrapping energy of deuterium from the trapping site and the trap density (which should be proportional to the irradiation defect density) are unknown, and were the free parameters in this simulation. The only kind of irradiation

defect was assumed to be the deuterium trapping site in this study for simplicity.

In this study, the distribution of irradiation defects was assumed as follows. In the case of 6.4 MeV Fe^{2+} irradiated tungsten, the irradiation defects are distributed within the implantation range. Also, several studies indicated that irradiation defect density would be saturated above the damage level of 0.2-0.4 dpa [26-28]. Therefore, the irradiation defect density in 6.4 MeV Fe^{2+} irradiated sample with the damage level of 0.3 dpa should be nearly saturated throughout the implantation range of 6.4 MeV Fe^{2+} in tungsten. Hence, the uniform defect density in 6.4 MeV Fe^{2+} irradiated tungsten up to 1.2 μm is initially considered. It should be noted that this damage level would decrease during deuterium gas absorption due to annealing of irradiation defects at high temperature, while the distribution of irradiation defects can be maintained [29]. For the precise simulation, the time evolution of irradiation defect density during deuterium gas absorption should be considered. In the simulation of this study, however, the irradiation defect density was assumed to be constant during deuterium gas absorption process. This assumption is justified by the quick saturation of deuterium in the absorption processes (see Section 4). Because the deuterium quickly fulfills the most of irradiation defects due to the high diffusivity along with the annealing of irradiation defect for 20 hours in total under 873 K, the consequent deuterium distribution should be uniform up to the implantation range of 6.4 MeV Fe^{2+} in tungsten. Hence, the uniform defect density in 6.4 MeV Fe^{2+} irradiated tungsten up to 1.2 μm is adopted in this simulation. The negligible defect density in the deeper region beyond 1.2 μm in this sample was also assumed.

For the case of neutron irradiated tungsten the uniform distribution of irradiation defects over the entire bulk of the sample was adopted because fast neutron can penetrate throughout 0.25 mm-thick tungsten. Also, the irradiation defect density would maintain during deuterium gas absorption process because the neutron irradiation temperature was much higher than that of deuterium gas absorption temperature.

The code consists of two stages. The first stage calculates the time-evolution of deuterium distribution in tungsten during deuterium gas exposure. In this step, the deuterium concentration on the top-surface of tungsten should be at equilibrium with deuterium gas. In this case, the deuterium surface concentration can be estimated by the relation of solubility [30-31]. The surface deuterium concentration changes with deuterium gas pressure and temperature. Therefore, the temperature history during deuterium gas exposure as shown in Fig. 1 was input into the code. The deuterium distribution at the end of deuterium gas exposure was used as the input data for the next stage.

The second stage of this code is the time-evolution of deuterium distribution in tungsten during TDS experiment. The decrease of deuterium retention at each time-step under elevating temperature with linear ramp rate gives the deuterium desorption rate from the sample in the TDS measurement. The temperature gradient within the sample during TDS measurement was not considered.

The above two-stage calculation was carried out with changing the detrapping energy and trap density to reproduce the deuterium retention and deuterium desorption spectrum (profile, peak-temperature, desorption rate at the peak).

4. Results and discussion

For the validation of the code, the deuterium migration in 6.4 MeV Fe^{2+} irradiated tungsten was analyzed first. Figure 2 show the results of TDS experiments for 6.4 MeV Fe^{2+} irradiated tungsten and un-damaged tungsten with deuterium gas absorption. The QMS signals for 6.4 MeV Fe^{2+} irradiated tungsten exhibits desorption of D_2, HD and HDO. The formation of HDO would be caused by the reaction of oxygen as a surface contaminant with deuterium that has migrated from the sub-surface. Also, the desorption peak of HD was slightly higher than that of D_2. In the TDS measurement, the background hydrogen signal increased in QMS with increasing the sample temperature because of the adsorbed hydrogen emission from the inner surface of TDS apparatus. The increase in background hydrogen in the TDS system should lead to the increase of the recombination efficiency of hydrogen and deuterium on the surface of tungsten. Therefore, desorption of HD tended to appear in higher temperature region than D_2. The total deuterium TDS spectrum for 6.4 MeV Fe^{2+} irradiated tungsten, which is shown in Fig. 2(b), is almost dominated by the desorption of D_2. The un-damaged tungsten is the same tungsten sample without ion/neutron irradiation, and was also exposed to D_2 gas in the same condition. In the case of un-damaged tungsten, a small deuterium desorption peak was found around 1000 K. It is reported that the intrinsic defects usually exist in tungsten, and influence on the migration of hydrogen isotopes [32-33]. Therefore, this deuterium desorption peak should be caused by the deuterium trapped by intrinsic defects which exist over the bulk of tungsten. Besides, the deuterium desorption peak appeared around 820 K in 6.4 MeV Fe^{2+} irradiated tungsten. This peak was not found in un-damaged tungsten, therefore, it should be caused by the deuterium trapping by irradiation defects induced by 6.4 MeV Fe^{2+} irradiation. 6.4 MeV Fe^{2+} irradiated tungsten showed a small deuterium desorption above 1000 K, and this should be caused by the intrinsic

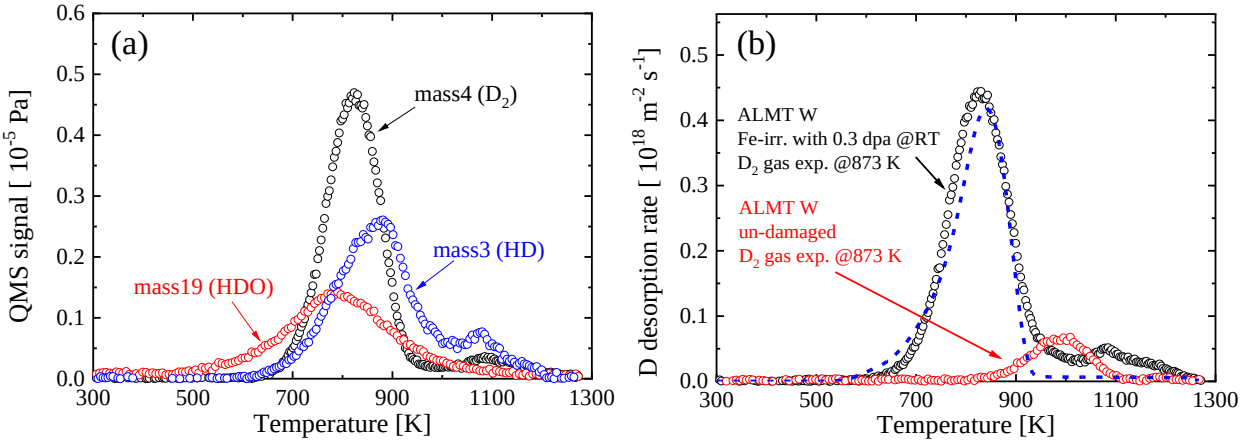

Fig. 2 The results of (a) QMS signals of several molecules containing deuterium in the TDS experiment for 6.4 MeV Fe^{2+} irradiated tungsten with deuterium gas absorption. The results of total deuterium TDS spectra for 6.4 MeV Fe^{2+} irradiated tungsten (black) and un-damaged tungsten (red) samples after deuterium gas absorption are also displayed in Fig. 2(b). The blue dashed line in Fig. 2(b) indicates the predicted deuterium desorption curve from the simulation code assuming the deuterium detrapping energy and the trap density as 1.85 eV and 0.6 at.%, respectively.

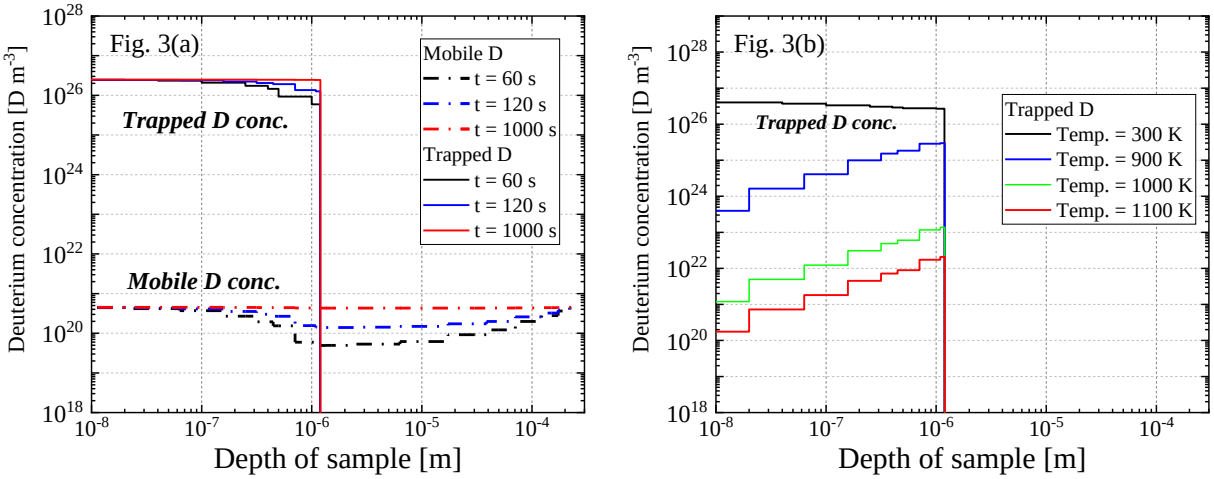

Fig. 3 Predicted deuterium distribution in 6.4 MeV Fe^{2+} irradiated tungsten (a) during deuterium gas absorption and (b) TDS measurement. Note that the concentration of mobile deuterium during TDS was much lower than 10^{18} m^{-3}, and is not displayed in this figure.

defects in the bulk of sample as in the case of un-damaged tungsten.

The predicted deuterium distribution in 6.4 MeV Fe^{2+} irradiated tungsten during D_2 gas absorption and TDS measurement are displayed in Figs. 3. The detrapping energy of deuterium from the trapping site and the trap density in this simulation were 1.85 eV and 0.6 at.%, respectively. This deuterium detrapping energy is similar to our previous study [24]. The localized distribution of trapped deuterium in irradiation defects are predicted within the depth of 1.2 μm, which corresponds to the implantation range of 6.4 MeV Fe^{2+} in tungsten. It was also predicted that deuterium retention in 6.4 MeV Fe^{2+} irradiated tungsten would be quickly saturated within a short time (~1000 s) of deuterium gas exposure. The predicted distribution of deuterium during TDS measurement showed that the deuterium concentration gradually decreased toward the surface with increasing temperature. The decrease of deuterium concentration in the sample with elevated temperature provides the TDS curve, and it is added in Figs. 2(b) as the blue dashed line. The overall deuterium desorption was reproduced by the simulation, indicating that the code used in this work is valid for estimating the deuterium migration in damaged tungsten.

Then, the analyses for neutron irradiated tungsten were carried out. Figure 4 shows the results of TDS experiments for neutron irradiated tungsten samples damaged by neutrons at 918 K and 1079 K, and then exposed to deuterium gas at 873 K. Figures 4(a) and 4(b) show the QMS signals for these samples. As in the case of 6.4 MeV Fe^{2+} irradiated tungsten, HD desorption became significant in higher temperature region. On the other hand, the desorption rate of HDO was relatively small in neutron irradiated tungsten because the amount of contaminant oxygen on the surface of tungsten would be limited while the deuterium retention was significantly

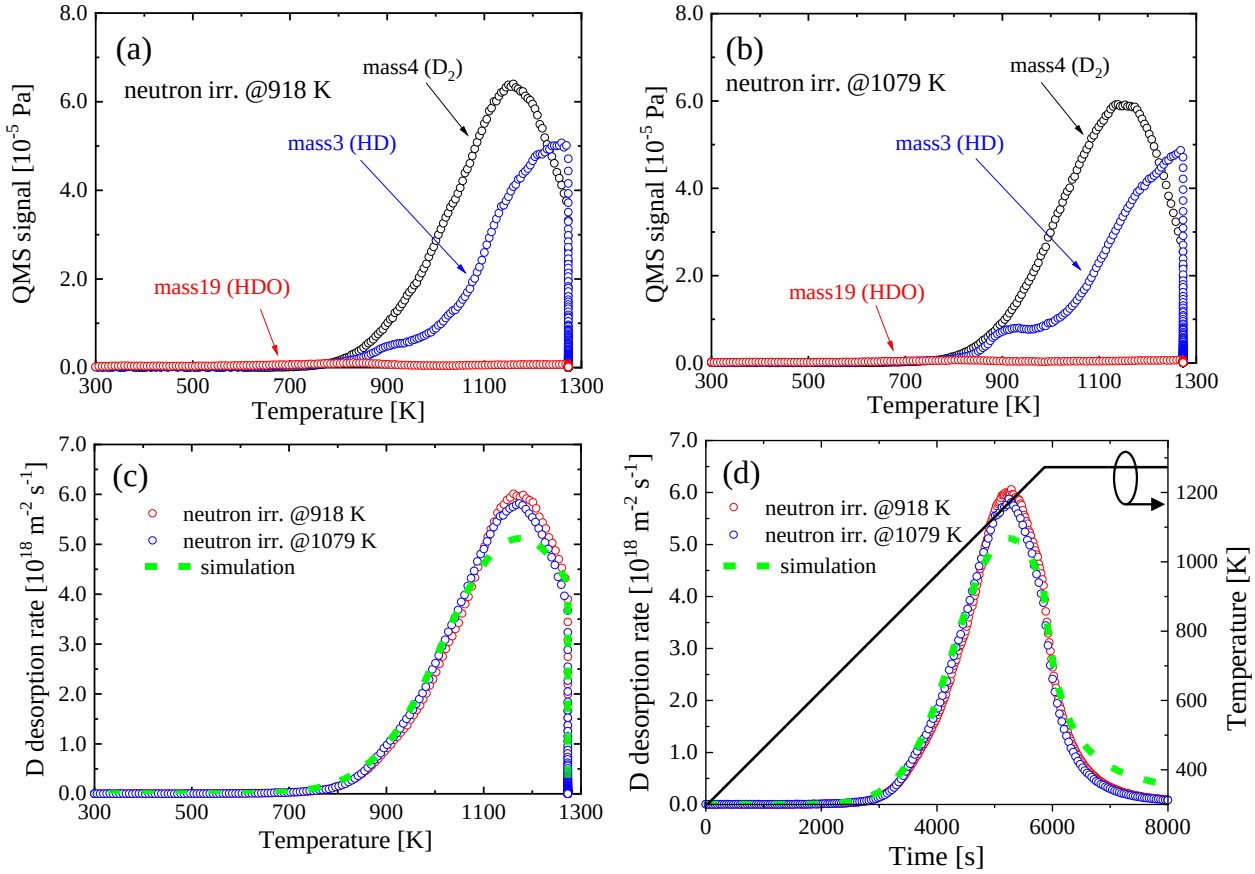

Fig. 4 The results of QMS signals of several molecules containing deuterium observed in the TDS measurements for neutron irradiated tungsten (a) damaged at 918 K (0.43 dpa) and (b) at 1079 K (0.74 dpa), then exposed to deuterium gas at 873 K for 20 hours in total. The results of total deuterium TDS spectra for these samples are also displayed (c) with respect to temperature, and (d) with respect to time and temperature. Green dashed lines indicate the predicted deuterium desorption curve from the simulation code assuming the deuterium detrapping energy and the trap density as 2.05 eV and 0.4 at.%, respectively.

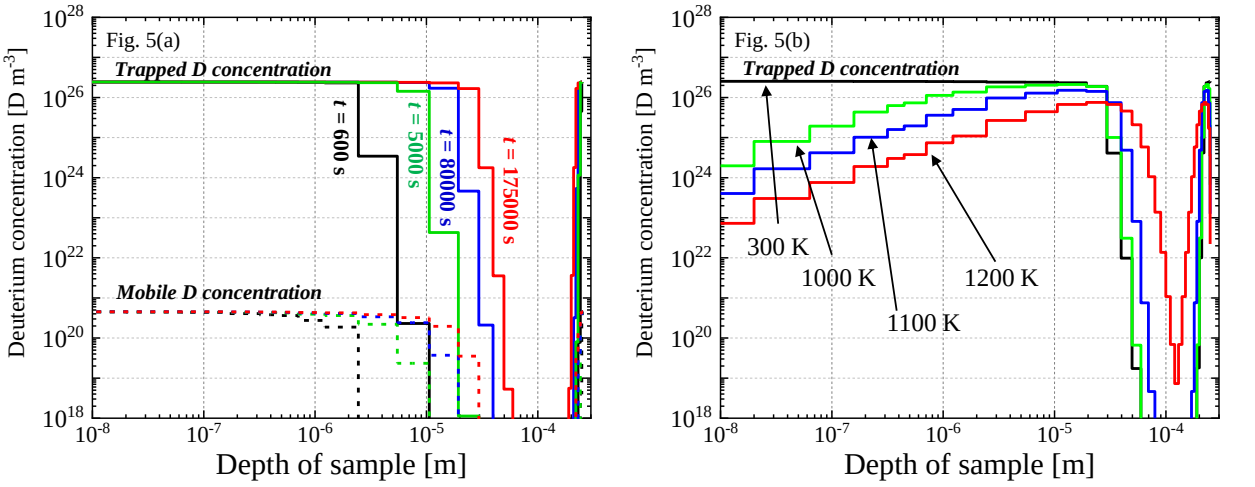

Fig. 5 Predicted deuterium distribution in neutron irradiated tungsten (a) during deuterium gas absorption and (b) TDS measurement. Note that the concentration of mobile deuterium during TDS was much lower than 10^{18} m^{-3}, and is not displayed in this figure.

higher in these samples compared to 6.4 MeV Fe^{2+} irradiated tungsten (see Figs. 4(c) and 4(d)).

The deuterium desorption rate with respect to temperature and that with respect to time and temperature are displayed in Figs. 4(c) and 4(d), respectively. The deuterium desorption rate significantly increased compared to that for 6.4 MeV Fe^{2+} irradiated tungsten due to the irradiation defects induced throughout the entire bulk of tungsten by neutron irradiation. Deuterium desorption had a peak at 1150 K, and deuterium desorption was still observed even after the temperature

rose to the maximum temperature of 1273 K in this study. By this continuous deuterium desorption rate after reaching at 1273 K, a drop in the deuterium desorption rate can be found in Fig. 4(c) at this temperature.

The predicted deuterium distribution in neutron irradiated tungsten during deuterium gas absorption and TDS are displayed in Figs. 5. The detrapping energy of deuterium from the trapping site and the trap density in this simulation were 2.05 eV and 0.4 at.%, respectively. The simulation results showed that deuterium occupies the trapping sites during its penetration into the bulk of tungsten because of a high detrapping energy of deuterium from the trapping sites. Therefore, it takes a long time to supply a sufficient amount of deuterium into tungsten during deuterium gas exposure, due to low hydrogen solution property of tungsten, to fulfill the trapping sites so that deuterium can penetrate throughout the bulk of tungsten. Consequently, it was predicted that the uniform distribution of deuterium throughout the bulk of neutron irradiated tungsten sample was hardly achieved by the deuterium gas exposure condition in this study. The predicted deuterium distribution during TDS showed that the deuterium concentration decreased toward the surface although that in the bulk region slightly increased with increasing temperature.

The simulated deuterium desorption curves for the neutron irradiated tungsten samples are also displayed in Figs. 4(c) and 4(d) as green dashed lines. The profile of deuterium desorption behavior and the deuterium retention were consistent with the experimental data assuming the detrapping energy and trap density as mentioned above. Note that the deuterium detrapping energy of 2.05 eV evaluated for the neutron irradiated tungsten was slightly higher than that of 6.4 MeV Fe^{2+} irradiated tungsten in which the deuterium detrapping energy was evaluated as 1.85 eV. It is well known that the irradiation defects can accumulate to form large-size defects [34-36]. The void which is formed by the accumulation of vacancies is the strong trapping site for hydrogen isotopes [34-40]. Also, it is reported that the stability of trapped hydrogen isotopes in voids can increase with the increase of the size of voids [13]. In the case of neutron irradiation, the irradiation temperature was high, and the irradiation duration was quite long compared to those of 6.4 MeV Fe^{2+} irradiation due to the high efficiency of irradiation defect production by heavy ion irradiation. Such high temperature and long duration under neutron irradiation would bring the migration of irradiation defects in tungsten. Therefore, the higher deuterium detrapping energy for neutron irradiated tungsten would suggest that deuterium is dominantly trapped by voids.

The assignment of the major deuterium trapping sites in neutron irradiated tungsten to voids can also be supported from the comparison of the deuterium TDS spectra for neutron irradiated tungsten samples with different irradiation temperatures and damage levels as shown in Figs. 4, where a slight difference on the deuterium desorption behavior was observed. A small difference in deuterium retention should indicate that the irradiation defect density is similar in these samples. A hint for understanding the similar irradiation defect density in these samples even with different neutron irradiation temperatures and damage levels is brought by the annealing behavior of irradiation defects in tungsten with elevated temperature. Anand reported electric resistance measurements for neutron irradiated tungsten. The results showed that the annealing of irradiation defects has specific recovery stages around 600 K and 1100 K [41], which can be assigned to the annealing of vacancies and voids, respectively [35-36]. This report suggested that voids do not significantly annealed up to 1100 K, and, therefore, can accumulate in tungsten in our neutron irradiation condition, where the nominal irradiation temperatures were 918 K (0.43 dpa) and 1079 K (0.74 dpa). Also, the density of trapped deuterium in irradiation defects in tungsten is usually saturated when the damage level is above 0.2-0.4 dpa [26-28]. Our samples experienced a fast neutron dose above the saturation level. As mentioned above, voids can be stable and accumulate even under 1079 K. Eventually, a similar irradiation defect density in neutron irradiated tungsten samples in this work is reasonable because the voids, which are stable below the irradiation temperature in this study, would accumulate in these samples.

Figure 4(d) also showed the relatively high deuterium desorption in the elapsed time above 6500 s, where the maximum temperature of TDS measurement was already achieved, compared to the experimental data. In the present simulation code, the annealing of irradiation defects is not considered. Therefore, the trap density was stable in TDS measurement. In the high temperature region, both detrapping rate and trapping rate of deuterium from/to the irradiation defects increased. Therefore, the deuterium desorption took a long time at high temperature due to the re-trapping of detrapped deuterium in the simulation. This influence was indeed observed in Fig. 5(b), where the deuterium concentration in the bulk region increased with increasing temperature. The irradiation defects distribute uniformly in the neutron irradiated tungsten, and it leads to a shift of deuterium desorption temperature toward higher temperature side as well as a large deuterium retention. Due to this characteristic of neutron irradiated tungsten, the annealing kinetics of irradiation defects are required to evaluate the migration behavior of hydrogen isotopes precisely, and therefore it should be studied in the near future.

Also, the effect of Gd thermal neutron absorber employed in this study was not discussed deeply here. Actually, this thermal neutron shield contributed to the lower radioactivity of samples to bring an easier handling of activated samples compared to the case of previous samples which required several years for cool down before the experiment. The different density of transmuted elements in tungsten may produce the changes in trap density and size of defect clusters, although comparable data carried out with the same condition to this study does not exist yet. The research to emphasize and reveal the effects of transmutation level in tungsten on hydrogen isotope migration behaviors will also be conducted in future.

5. Conclusion

Deuterium was introduced into neutron damaged tungsten and 6.4 MeV Fe^{2+} damaged tungsten by means of gas absorption method in this study. The deuterium desorption spectra for tungsten samples were analyzed by a numerical model which includes the elementary steps of hydrogen isotope migration such as diffusion, trapping, detrapping, and so on. The results can be summarized as follows.

- In the case of 6.4 MeV Fe^{2+} irradiated tungsten sample, the desorption spectrum of deuterium trapped by irradiation defects was almost reproduced assuming the detrapping energy and trap density as 1.85 eV and 0.6 at.%, respectively. The estimated deuterium distribution during deuterium gas absorption suggested that irradiation defects would be occupied by deuterium quickly.
- Tungsten samples damaged by neutron under 918 K and 1079 K up to 0.43 dpa and 0.74 dpa, respectively, showed the similar deuterium desorption spectra. Deuterium retention in neutron irradiated tungsten sample was significantly higher than that of 6.4 MeV Fe^{2+} irradiated tungsten sample because the irradiation defects should generate throughout the bulk of tungsten by neutron irradiation. The predicted deuterium distribution assuming the detrapping energy of 2.05 eV and trap density of 0.4 at.% showed that the uniform deuterium distribution throughout an entire depth of tungsten sample hardly achieved in the present experimental condition. The deuterium desorption spectra could be reproduced by the simulation using the above parameters of trapping/detrapping. The voids would be the dominant deuterium trapping site in neutron irradiated tungsten.
- The research to understand the annealing of irradiation defects is more important for analyzing deuterium migration behaviors in neutron irradiated tungsten because deuterium trapping/detrapping rates are emphasized at elevated temperature, and simultaneously, irradiation defect will annihilate in such a high temperature.

Acknowledgments

This material is based upon work supported by the U.S. Department of Energy Office of Science, Office of Fusion Energy Sciences, under the DOE Idaho Operations Office contract number DE-AC07-05ID14517 and under the UT-Battelle, LLC. contract DE-AC05-00OR22725.

This work was supported by a Japan-US collaboration research program, PHENIX, and JSPS Kakenhi No.17K14901.

References

[1] O.V. Ogorodnikova, Surface effects on plasma-driven tritium permeation through metals, J. Nucl. Mater., 290 (2001) 459.

[2] Y. Ueda et al., Research status and issues of tungsten plasma facing materials for ITER and beyond, Fusion Eng. Des., 89 (2014) 901-906.

[3] M. Kobayashi et al., Trapping behaviour of deuterium ions implanted into tungsten simultaneously with carbon ions, Phys. Scr., T138 (2009) 014050T.

[4] M. Rieth et al., Behavior of tungsten under irradiation and plasma interaction, J. Nucl. Mater., 519 (2019) 334-368.

[5] T. Tanabe et al., Review of hydrogen retention in tungsten, Phys. Scr., T159 (2014) 014044.

[6] T. Otsuka and T. Tanabe, Application of a tritium imaging plate technique to depth profiling of hydrogen in metals and determination of hydrogen diffusion coefficients, Mater Transact., 58 (2017) 1364-1372.

[7] M. Shimada et al., First result of deuterium retention in neutron-irradiated tungsten exposed to high flux plasma in TPE, J. Nucl. Mater., 415 (2011) S667.

[8] Y. Hatano et al., Trapping of hydrogen isotopes in radiation defects formed in tungsten by neutron and ion irradiations, J. Nucl. Mater., 438 (2013) S114-S119.

[9] Y. Hatano et al., Deuterium trapping at defects created with neutron and ion irradiations in tungsten, Nucl. Fusion, 53 (2013) 073006.

[10] Y. Oya et al., Interaction of hydrogen isotopes with radiation damaged tungsten, Adv. Intell. Syst. Com-put. 660 (2017) 41-49.

[11] C. Bellecci et al., Loss of vacuum accident (LOVA): Comparison of computational fluid dynamics (CFD) flow velocities against experimental data for the model validation, Fusion Eng. Des., 86 (2011) 330-340.

[12] T. Honda et al., Analyses of loss of vacuum accident (LOVA) in ITER, Fusion Eng. Des., 47 (2000) 361-375.

[13] Y. Oya et al., D retention and depth profile behavior for single crystal tungsten with high temperature neutron irradiation, J. Nucl. Mater., 539 (2020) 152323.

[14] V. Kh. Alimov et al., Depth distribution of deuterium in single- and polycrystalline tungsten up to depths of several micrometers, J. Nucl. Mater., 337–339 (2005) 619–623.

[15] J.B. Condon, T. Schober, Hydrogen bubbles in metals, J. Nucl. Mater. 207 (1993) 1-24.

[16] L.M. Garrison, et al., Phenix U.S.-Japan collaboration investigation of thermal and mechanical properties of thermal neutron–shielded irradiated tungsten, Fusion Sci. Technol., 75 (2019) 499-509.

[17] K. Hoshino et al., Progress of Divertor Study on DEMO Design, Plasma and Fusion Rsearch, 12 (2017) 1405023.

[18] M. Shimada et al., Hydrogen Isotope Retention and Permeation in Neutron-Irradiated Tungsten and Tungsten Alloys Under PHENIX Collaboration, Fusion Sci. Technol., 72 (2017) 652-659.

[19] A. Kohyama et al., A new Multiple Beams–Material Interaction Research Facility for radiation damage studies in fusion materials, J. Nucl. Mater., 51-52 (2000) 789-795.

[20] M. Kobayashi et al., Deuterium trapping by irradiation damage in tungsten induced by different displacement processes, Fusion Eng. Des. 88 (2013) 1749-1752.

[21] J.F. Ziegler, <http://www.srim.org/>.
[22] H. Zhang et al., Characterization of tritium isotopic permeation through ARAA in diffusion limited and surface limited regimes., Fusion Sci. Technol., 72 (2017) 416-425.
[23] R.A. Anderl et al., Deuterium Transport and Trapping in Polycrystalline Tungsten, Fusion Technol., 21 (1992), p. 745.
[24] M. Kobayashi et al., Influence of dynamic annealing of irradiation defects on the deuterium retention behaviors in tungsten irradiated with neutron, Fusion Eng. Des., 146 (2019) 1624-1627.
[25] M. Kobayashi and Y. Oya, Development of the Tritium Transport Model for Pebbles of Li_2TiO_3, Plasma Fusion Res., 13 (2018) 3405048.
[26] O.V. Ogorodnikova et al., The influence of radiation damage on the plasma-induced deuterium retention in self-implanted tungsten, J. Nucl. Mater., 415 (2011) S661.
[27] O.V. Ogorodnikova and V. Gann, Simulation of neutron-induced damage in tungsten by irradiation with energetic self-ions, J. Nucl. Mater., 460 (2015) 60-71.
[28] B. Tyburska et al., Deuterium retention in self-damaged tungsten, J. Nucl. Mater., 395 (2009) 150-155.
[29] Y. Hatano et al., Deuterium retention in W and W-Re alloy irradiated with high energy Fe and W ions: Effects of irradiation temperature, Nucl. Mater. Energy, 9 (2016) 93-97.
[30] R. Frauenfelder, Solution and Diffusion of Hydrogen in Tungsten, J. Vac. Sci. Technol., 6 (1969) 388.
[31] G.R. Longhurst, D.F. Holland, J.L. Jones, B.J. Merrill, TMAP4 User's Manual, EGG-FSP-10315, DOI: 10.2172/7205576.
[32] J. Roth and K. Schmid, Hydrogen in tungsten as plasma-facing material, Phys. Scr. T145, 014031 (2011).
[33] C.S. Becquat et al., Microstructural evolution of irradiated tungsten: Ab initio parameterisation of an OKMC model, J. Nucl. Mater., 403 (2010) 75-88.
[34] O.V. Ogorodnikova et al., Annealing of radiation-induced damage in tungsten under and after irradiation with 20 MeV self-ions, J. Nucl. Mater., 451 (2014) 379-386.
[35] S. Sakurada et al., Annealing effects on deuterium retention behavior in damaged tungsten, Nucl. Mater. Energy, 9 (2016) 141-144.
[36] M. Poon et al., Modelling deuterium release during thermal desorption of D+-irradiated tungsten, J. Nucl. Mater. 374, 390 (2008).
[37] Z. Wang et al., fusengdesModeling of fuel retention and hydrogen-isotope exchange removal from thepre-damaged tungsten material, Fusion Eng. Des., 136 (2018) 372-376.
[38] M. Zibrov et al., High temperature recovery of radiation defects in tungsten and its effect on deuterium retention, Nucl. Mater. Energy, 23 (2020) 100747.
[39] Y. Jin et al., Enhancement of deuterium retention in damaged tungsten by plasma-induced defect clustering, Nucl. Fusion., 57 (2017) 126042.
[40] M.H.J. 't Hoen, et al., Reduced deuterium retention in self-damaged tungsten exposed to high-flux plasmas at high surface temperatures, Nucl. Fusion 53 (2013) 043003.
[41] M.S. Anand et al., Recovery in neutron irradiated tungsten, Radiation Effects, 39 (1978) 149-155.